Universal Probability Distributions of Scattering Observables in Ultracold Molecular Collisions

Masato Morita,[1] Roman V. Krems,[2] and Timur V. Tscherbul[1]
[1]Department of Physics, University of Nevada, Reno, Nevada 89557, USA
[2]Department of Chemistry, University of British Columbia, Vancouver, British Columbia V6T 1Z1, Canada

(Received 7 December 2018; revised manuscript received 9 May 2019; published 2 July 2019)

Currently, quantum dynamics theory cannot be used for quantitative predictions of molecular scattering observables at low temperatures because of two problems. The first problem is the extreme sensitivity of the low-temperature observables to details of potential energy surfaces (PESs) parametrizing the nuclear Schrödinger equation. The second problem is the large size of the basis sets required for the numerical integration of the Schrödinger equation for strongly interacting molecules in the presence of fields, which precludes the application of rigorous quantum theory to all but a few atom-molecule systems. Here, we show that, if the scattering problem is formulated as a probabilistic prediction, quantum theory can provide reliable results with exponentially reduced numerical effort. Specifically, we show that the probability distributions that an observable is in a certain range of values can be obtained by averaging the results of scattering calculations with much smaller basis sets than required for calculations of individual scattering cross sections. Moreover, we show that such distributions do not rely on the precise knowledge of the PES. This opens the possibility of making probabilistic predictions of experimentally relevant observables for a wide variety of molecular systems, currently considered out of reach of quantum dynamics theory. We demonstrate the approach by computing the probability for elastic scattering of CaH and SrOH molecules by Li atoms and SrF molecules by Rb atoms.

DOI: 10.1103/PhysRevLett.123.013401

Molecular collisions are at the core of experiments with ultracold molecules [1–4], which form the foundation for multiple, rapidly evolving research fields, ranging from cold controlled chemistry [5] to quantum computing with trapped molecules [6] to quantum simulation [2,3] and precision tests of fundamental symmetries [1,2,5,7]. Recent highlights include the production of high-phase-space-density ensembles of polar radicals SrF($^2\Sigma$) and CaF($^2\Sigma$) via laser cooling and magnetic trapping [8,9], fundamental studies of ultracold molecular collisions and chemical reactions in the single partial-wave regime [10,11], external field control of reaction dynamics [12–14] and stereodynamics [15], the observation of dipolar exchange interactions between ultracold KRb molecules trapped in an optical lattice [16], and order-of-magnitude better limits on the electric dipole moment of the electron [17]. In addition, ultracold molecular collisions provide new insights into quantum chaos and its relation to quantum scattering [18–21].

As molecular phase-space densities continue to increase toward quantum degeneracy, it is increasingly more important to understand molecular collisions at low temperatures. This is required for controlling molecular interactions with external fields [4,22], which is a necessary ingredient in many applications of ultracold molecular gases [1]. Collisions are essential for cooling experiments. While momentum energy transfer in elastic collisions enables sympathetic and/or evaporative cooling, inelastic collisions lead to undesirable trap loss and heating. A large ratio of elastic-to-inelastic collision rates ($\gamma \geq 100$) is among the key factors that determine the feasibility of cooling experiments [1,23]. Collisions also limit precision measurements. Finally, understanding molecular collisions is critically important for the development of the primary pressure standard for high- and ultrahigh-vacuum regimes [24–27]. Quantum scattering calculations of molecular collisions are essential to guide experiments in the choice of molecular systems amenable to collisional cooling, control, and applications of cold molecules. However, at present, quantum scattering calculations cannot be used for quantitative predictions of molecular collision observables at ultracold temperatures for two reasons.

First, low-temperature scattering observables are extremely sensitive to small uncertainties in the potential energy surface (PES) underlying quantum scattering calculations [28–31]. This well-known phenomenon is illustrated in Fig. 1, showing the variation of scattering cross sections with a scaling factor modifying the PES for a relatively simple Li-CaH collision system. As can be seen, a small variation (<1%) of the PES may change the scattering cross sections by as much as 10 orders of magnitude. This characteristic phenomenon is a result of the presence of a large number of scattering resonances that emerge at zero energy as the potential is scaled. The uncertainty of the PES produced by current quantum

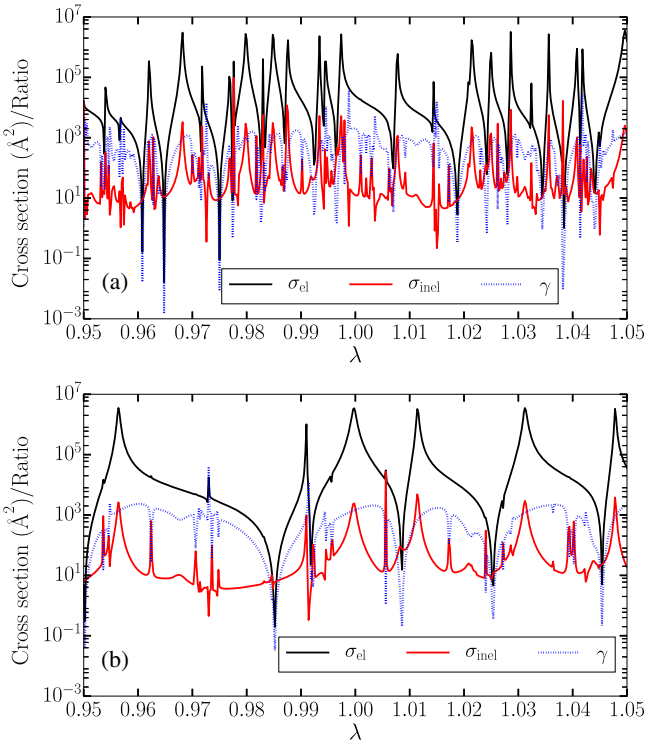

FIG. 1. Elastic cross section σ_{el} (black solid), inelastic cross section σ_{inel} (red solid), and the ratio of elastic-to-inelastic cross sections γ (blue dashed) as a function of the potential scaling parameter λ for Li-CaH at the collision energy of $E_C = 10^{-5}$ cm^{-1} with the external magnetic field of 100 G for (a) $N_{max} = 55$ and (b) $N_{max} = 5$.

chemistry methods, especially for heavy open-shell systems of relevance to the research field of ultracold molecules [8,9,32,33], is much larger than 1%. As a result, even for the lightest collision systems [10], it is not presently possible to determine cold collision cross sections with quantitative accuracy [13,34–36].

The second major problem making quantum predictions of ultracold scattering observables unfeasible is that of basis set convergence. Molecular interactions are strongly anisotropic and couple a large number of rotational, fine, and hyperfine states. As a result, quantum scattering calculations of ultracold collision properties must include a very large number of basis functions [13,34,37] to achieve numerical convergence, severely limiting the scope of ultracold collision problems amenable to a rigorous theoretical study.

In this Letter, we propose a new statistical approach to overcome both of the central problems in ultracold molecular collision theory. We argue that the results displayed in Fig. 1 contain meaningful statistical information, which can be used to predict the probability of scattering events. In particular, we show that an ensemble of scattering results with different PESs could be characterized by the cumulative probability distributions (CPDs), which appear to be universal to different basis sets and can thus be obtained with high precision based on scattering calculations with small basis sets. This is critically important, as this opens up the possibility of making predictions of experimentally relevant observables for a wide variety of molecular systems, currently considered out of reach of quantum dynamics theory.

As a first application, we calculate the CPDs for cold Li-CaH, Li-SrOH, and Rb-SrF collisions in a magnetic field to estimate the probability of a large elastic-to-inelastic cross section ratio $P(\gamma > 100)$. The elastic scattering probability is an essential figure of merit for molecular sympathetic cooling [38–40]. We show that the CPDs of the elastic-to-inelastic ratio γ provide a natural way to estimate the probability, leading to an efficient methodology for screening molecular candidates with favorable collisional properties for sympathetic cooling.

We begin by defining the CPD of a scattering observable γ, which we assume to be a random variable drawn from an ensemble $\{\gamma_i\}$ (in the following γ will be identified with the elastic-to-inelastic ratio)

$$F(\Gamma) = P(\gamma \leq \Gamma), \tag{1}$$

where $P(\gamma \leq \Gamma)$ is the probability that γ does not exceed Γ. In the limit of infinitely large ensemble size, the CPD may be expressed as $F(\Gamma) = \int_0^\Gamma p(\gamma) d\gamma$, where $p(\gamma)$ is the probability density function of the observable γ. Assuming that an atom-molecule collision pair is suitable for sympathetic cooling if $\gamma > 100$ [1], we can define the "elastic scattering probability" as $P_s = 1 - F(\Gamma = 100)$, which represents the fraction of the elements in the ensemble for which $\gamma > 100$.

To obtain the statistics of scattering observables necessary to evaluate the CPD, we sample the interaction PES V using the potential scaling method, whereby the atom-molecule PES is multiplied by a dimensionless scaling factor λ, which is varied to introduce the PES uncertainty [30,39,41–43]. We scan the value of λ from 0.95 to 1.05 with the grid step $\Delta\lambda = 2 \times 10^{-4}$, leading to a sample of 501 points $\{V_i\}$ $(i = 1, 2, \ldots, 501)$, drawn from the ensemble with $\pm 5\%$ uncertainty, which corresponds to a typical accuracy of modern *ab initio* PESs [39]. For V, we use the accurate *ab initio* interaction PESs for Li-CaH, Li-SrOH, and Rb-SrF from our previous work [40,44,45]. We note that the precise estimate of the uncertainty is not important for our statistical approach, as shown in the Supplemental Material [46–51]. By carrying out coupled-channel (CC) calculations for every V_i in $\{V_i\}$ as described below, we obtain samples of scattering observables such as the elastic $\{\sigma_{el,i}\}$ and inelastic $\{\sigma_{inel,i}\}$ cross sections and their ratio $\{\gamma_i\}$. We note that more elaborate random sampling methods produce essentially the same CPDs as the standard λ-scaling method used here [46].

Having specified the potential ensembles, we proceed to carry out numerically exact quantum scattering calculations

on ultracold collisions of alkali-metal atoms (A) with $^2\Sigma^+$ radicals (B) in the presence of an external magnetic field. In atomic units, the Hamiltonian of the collision complex is [44,45]

$$\hat{\mathcal{H}} = -\frac{1}{2\mu R}\frac{d^2}{dR^2}R + \frac{(\hat{J}-\hat{N}-\hat{S}_A-\hat{S}_B)^2}{2\mu R^2} + \hat{\mathcal{H}}_A + \hat{\mathcal{H}}_B + \hat{\mathcal{H}}_{\rm int}, \tag{2}$$

where R is the distance between the atom and the center of mass of the molecule, μ and $\hat{J}$ are the reduced mass and the total angular momentum of the collision complex, $\hat{N}$ is the rotational angular momentum of the molecule, and $\hat{S}_A$ and $\hat{S}_B$ are the atomic and molecular spins. The atomic Hamiltonian $\hat{\mathcal{H}}_A = g_e\mu_B\hat{S}_{A,Z}B$, where g_e is the electron g factor, μ_B is the Bohr magneton, $\hat{S}_{A,Z}$ is the projection of $\hat{S}_A$ onto the magnetic field axis, and B is the magnitude of the external magnetic field. The molecular Hamiltonian $\hat{\mathcal{H}}_B = B_e\hat{N}^2 + \gamma_{\rm SR}\hat{N}\cdot\hat{S}_B + g_e\mu_B\hat{S}_{B,Z}B$, where B_e and $\gamma_{\rm SR}$ are the rotational and spin-rotation constants. In Eq. (2), $\hat{\mathcal{H}}_{\rm int} = \lambda\hat{V} + \hat{V}_{\rm dd}$ is the atom-molecule interaction, where $\hat{V}$ is the scaled atom-molecule PES discussed above and $\hat{V}_{\rm dd}$ is the magnetic dipole-dipole interaction [45]. The wave function of the collision complex is expanded in a set of basis functions [40,44,52] $|JM\Omega\rangle|NK_N\rangle|S_A\Sigma_A\rangle|S_B\Sigma_B\rangle$, where Ω, K_N, Σ_A, and Σ_B are the projections of J, N, S_A, and S_B onto the body-fixed z axis defined by the atom-diatom Jacobi vector $\mathbf{R}$, leading to a system of CC equations, which is solved numerically as described in our previous work [40,44–46,52]. The size of the basis set is determined by the cutoff parameters $J_{\rm max}$ and $N_{\rm max}$, which give the maximum values of J and N. Using $J_{\rm max} = 3$ gives converged results over the collision energy range studied here ($E_C = 10^{-6} - 10^{-2}$ cm^{-1}). We consider ultracold collisions of rotationally ground-state molecules in their maximally stretched low-field-seeking Zeeman states with spin-polarized alkali-metal atoms.

In Fig. 2, we show the CPDs of the scattering cross sections for Li-CaH, Li-SrOH, and Rb-SrF obtained in CC calculations with different basis sets. Remarkably, the CPDs converge quickly with respect to basis set size, as shown for Li-CaH in Figs. 2(a1) and 2(a2). This demonstrates that we can obtain accurate CPDs using severely restricted CC basis sets that would be too small to produce fully converged scattering cross sections. This opens up the prospect of computing accurate CPDs for more complex molecular systems, for which fully converged CC calculations are prohibitively difficult.

From Fig. 2(a2), the probability for the elastic-to-inelastic ratio γ to fall below 100 is ~0.2, giving the elastic scattering probability of 80%. This probability, as derived from the CPD, thus provides a useful parameter for screening the suitability of atom-molecule systems for sympathetic cooling based on their collisional properties. The rapid convergence of CPDs with respect to $N_{\rm max}$ is an important advantage of the CPDs over the individual γ values used previously for this purpose [1,40,53].

Figures 2(b1) and 2(b2) show the results for a heavier collision system Li-SrOH, which requires much larger rotational basis sets than Li-CaH ($N_{\rm max} = 115$) to obtain

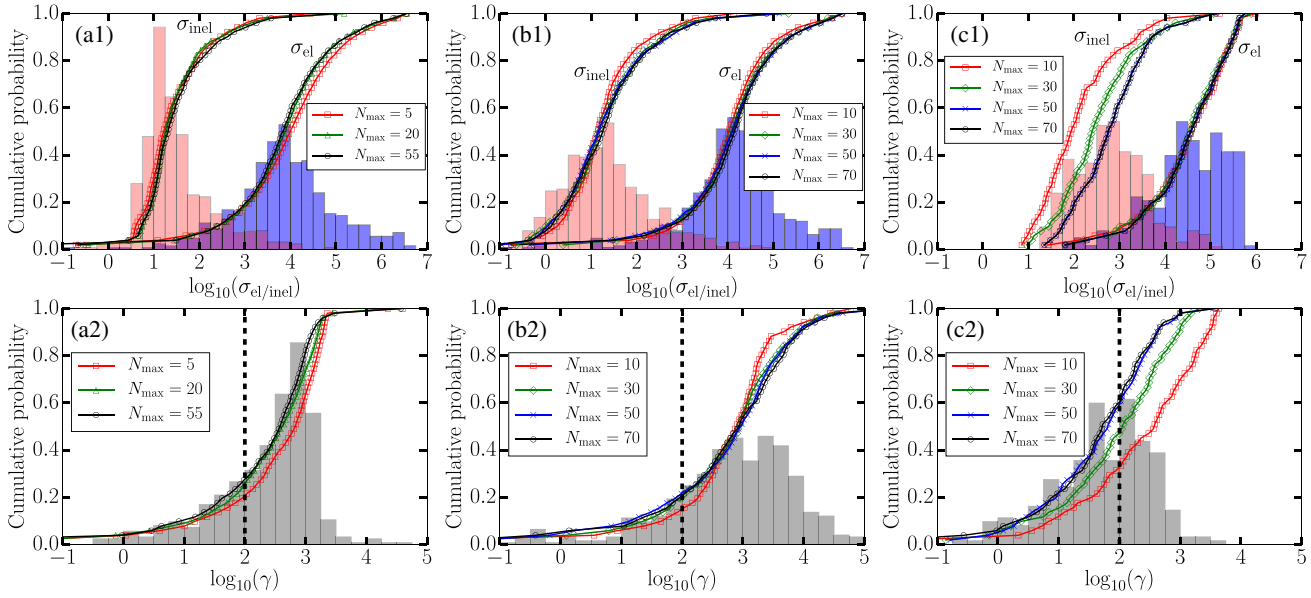

FIG. 2. $N_{\rm max}$ dependence of the cumulative probability distributions of elastic $\sigma_{\rm el}$ and inelastic $\sigma_{\rm inel}$ cross sections in Å^2 (upper) and the ratio of elastic-to-inelastic cross sections γ (lower) for (a) Li-CaH, (b) Li-SrOH, and (c) Rb-SrF at the collision energy of 10^{-5} cm^{-1} with the external magnetic field of 100 G. Normalized histograms show the distributions of the observables obtained with the largest $N_{\rm max}$ values in each panel. At the limit of infinitely large sample size, the histograms would converge to the probability densities.

converged results, due to the small rotational constant of SrOH [45,46]. Despite this, we observe rapid convergence of the CPDs with respect to $N_{\max}$, making it possible to use basis sets with $N_{\max} = 30$ for quantitatively accurate calculations.

The physical reason behind the rapid basis set convergence of the CPDs is that the ensemble-averaging procedure washes out the intricate details of the resonance structure shown in Fig. 1, provided that the λ interval contains enough resonances, which is ensured by the high resonance density. We note that the CPDs do not contain information about the correlation between the values of λ and those of the scattering observables. For example, if we consider a periodic function of λ, the CPD of the periodic function is invariant with respect to the change of the period of oscillations as long as the function oscillates many times in the chosen interval of λ. Thus, while we observe a significant difference in the resonance density as a function of λ between Figs. 1(a) and 1(b), such differences tend to have no effect on the CPDs.

Figure 2(c1) shows the CPDs calculated for the heaviest collision system studied here (Rb-SrF), which also exhibits the slowest basis set convergence, with $N_{\max} = 125$ required to produce accurate results [44]. The CPDs of the inelastic cross sections (but not the elastic ones) tend toward higher values of σ_{inel} with increasing $N_{\max}$, saturating only at $N_{\max} = 50$, which is still significantly lower than required for the fully converged CC calculation [44]. We attribute the slow convergence rate to the broad shape resonances that occur in the inelastic cross sections [44], affecting their background values over a large range of magnetic fields. This also indicates that the couplings with very highly excited rotational channels $N > 30$ play an important role for the background value of the inelastic cross section due to the strong anisotropy of the Rb-SrF interaction.

To explore the variation of the CPDs with the collision energy and magnetic field, we compare in Fig. 3(a) the CPDs of the elastic-to-inelastic ratio γ for Li-CaH in the s-wave regime ($E_C = 10^{-5}$ cm^{-1}) vs the multiple partial-wave regime ($E_C = 10^{-3}$ cm^{-1}). Figure 3(b) shows a similar plot for two different values of the magnetic field. We observe that the CPDs at different collision energies and magnetic fields are statistically distinguishable from each other, even within the limits imposed by numerical convergence, making it possible to reliably predict the variation of the elastic scattering probability with collision energy and field. The results shown in Fig. 3 also suggest that the rapid convergence of CPDs with respect to $N_{\max}$ holds regardless of the collision energy and magnetic field. We can therefore systematically examine the success probability of sympathetic cooling as a function of these parameters using modest basis sets.

Figure 4 shows the elastic scattering probability for Li-CaH as a function of collision energy. At $E_C \sim 1$ mK,

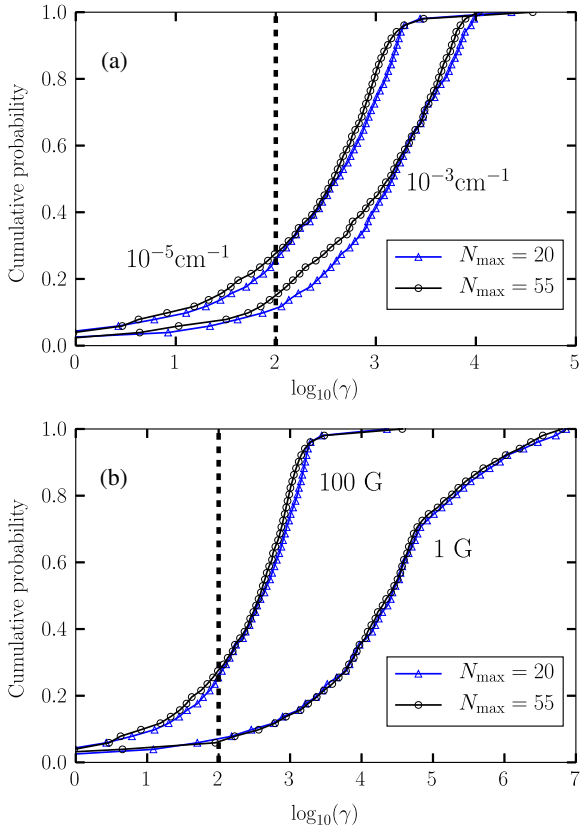

FIG. 3. Comparison of the cumulative probability distributions of the elastic-to-inelastic ratio for Li-CaH (a) between $E_C = 10^{-5}$ and $E_C = 10^{-3}$ cm^{-1} with the external magnetic field of 100 G and (b) between $B = 100$ vs $B = 1$ G at the collision energy of 10^{-5} cm^{-1}.

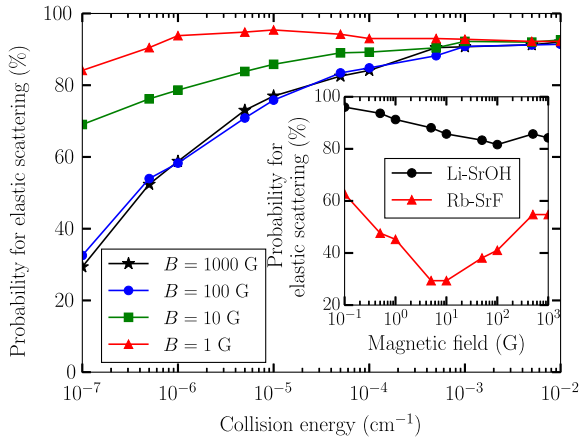

FIG. 4. Elastic scattering probability for Li-CaH as a function of collision energy for the external magnetic field of 1000 G (black stars), 100 G (blue circles), 10 G (green squares), and 1 G (red triangles). $N_{\max} = 20$. Inset: Same for Li-SrOH (black circles) and Rb-SrF (red triangles) as a function of magnetic field at the collision energy of 10^{-5} cm^{-1}. $N_{\max} = 30$ for Li-SrOH and $N_{\max} = 50$ for Rb-SrF.

the probability is high regardless of the magnitude of the magnetic field, but decreases significantly with decreasing collision energy due to the Wigner threshold dependence of the elastic-to-inelastic ratio for s-wave scattering ($\gamma \propto E_C^{1/2}$). At lower collision energies, the probability decreases by a factor of ~3 with increasing field due to increased field sensitivity of the inelastic cross sections caused by numerous scattering resonances, which tend to enhance inelastic cross sections without affecting elastic scattering [44]. A significant magnetic field dependence of the elastic probability for Rb-SrF shown in the inset of Fig. 4 suggests that varying the field could be used to optimize sympathetic cooling of $^2\Sigma$ molecules with alkali-metal atoms in a magnetic trap [44].

In summary, we have proposed a new statistical approach to account for the effect of PES uncertainties on cold collision observables. The approach is based on the CPDs computed by averaging the results of quantum scattering calculations over an ensemble of interaction PESs produced by the potential scaling method. The remarkably fast basis set convergence of the CPDs makes our approach applicable to a wide range of molecular collision systems of current experimental interest, such as ultracold chemical reactions [13] and polyatomic molecules SrOH and CH_3 with their low-frequency vibrational modes [32,54], which are challenging to describe at the rigorous converged coupled-channel level (although the quantum scattering methodology capable of treating the vibrational modes has yet to be developed). It would be interesting to further explore the properties of CPDs in connection with the statistical model of insertion chemical reactions [20,55] and with the theory of quantum chaotic scattering [18,19,21].

We are grateful to Balakrishnan Naduvalath for stimulating discussions. This work was supported by NSF Grant No. PHY-1607610.

[1] L. D. Carr, D. DeMille, R. V. Krems, and J. Ye, New J. Phys. **11**, 055049 (2009).
[2] J. L. Bohn, A. M. Rey, and J. Ye, Science **357**, 1002 (2017).
[3] S. A. Moses, J. P. Covey, M. T. Miecnikowski, D. S. Jin, and J. Ye, Nat. Phys. **13**, 13 (2017).
[4] R. V. Krems, *Molecules in Electromagnetic Fields: From Ultracold Physics to Controlled Chemistry* (Wiley, New York, 2018).
[5] R. V. Krems, Phys. Chem. Chem. Phys. **10**, 4079 (2008).
[6] D. DeMille, Phys. Rev. Lett. **88**, 067901 (2002).
[7] M. S. Safronova, D. Budker, D. DeMille, Derek F. Jackson Kimball, A. Derevianko, and C. W. Clark, Rev. Mod. Phys. **90**, 025008 (2018).
[8] D. J. McCarron, M. H. Steinecker, Y. Zhu, and D. DeMille, Phys. Rev. Lett. **121**, 013202 (2018).
[9] L. Anderegg, B. L. Augenbraun, Y. Bao, S. Burchesky, L. W. Cheuk, W. Ketterle, and J. M. Doyle, Nat. Phys. **14**, 890 (2018).
[10] A. Klein, Y. Shagam, W. Skomorowski, P. S. Żuchowski, M. Pawlak, L. M. C. Janssen, N. Moiseyev, S. Y. T. van de Meerakker, A. van der Avoird, C. P. Koch, and E. Narevicius, Nat. Phys. **13**, 35 (2017).
[11] W. E. Perreault, N. Mukherjee, and R. N. Zare, Science **358**, 356 (2017).
[12] K. K. Ni, S. Ospelkaus, D. Wang, G. Quéméner, B. Neyenhuis, M. H. G. de Miranda, J. L. Bohn, J. Ye, and D. S. Jin, Nature (London) **464**, 1324 (2010).
[13] N. Balakrishnan, J. Chem. Phys. **145**, 150901 (2016).
[14] T. V. Tscherbul and R. V. Krems, Phys. Rev. Lett. **115**, 023201 (2015).
[15] M. H. G. de Miranda, A. Chotia, B. Neyenhuis, D. Wang, G. Quéméner, S. Ospelkaus, J. L. Bohn, J. Ye, and D. S. Jin, Nat. Phys. **7**, 502 (2011).
[16] B. Yan, S. A. Moses, B. Gadway, J. P. Covey, K. R. A. Hazzard, A. M. Rey, D. S. Jin, and J. Ye, Nature (London) **501**, 521 (2013).
[17] V. Andreev, D. G. Ang, D. DeMille, J. M. Doyle, G. Gabrielse, J. Haefner, N. R. Hutzler, Z. Lasner, C. Meisenhelder, B. R. O'Leary, C. D. Panda, A. D. West, E. P. West, and X. Wu (ACME Collaboration), Nature (London) **562**, 355 (2018).
[18] A. Frisch, M. Mark, K. Aikawa, F. Ferlaino, J. L. Bohn, C. Makrides, A. Petrov, and S. Kotochigova, Nature (London) **507**, 475 (2014).
[19] J. F. E. Croft and J. L. Bohn, Phys. Rev. A **89**, 012714 (2014).
[20] J. F. E. Croft, C. Makrides, M. Li, A. Petrov, B. K. Kendrick, N. Balakrishnan, and S. Kotochigova, Nat. Commun. **8**, 15897 (2017).
[21] M. Mayle, G. Quéméner, B. P. Ruzic, and J. L. Bohn, Phys. Rev. A **87**, 012709 (2013).
[22] M. Lemeshko, R. V. Krems, J. M. Doyle, and S. Kais, Mol. Phys. **111**, 1648 (2013).
[23] J. Lim, M. D. Frye, J. M. Hutson, and M. R. Tarbutt, Phys. Rev. A **92**, 053419 (2015).
[24] J. L. Booth, P. Shen, R. V. Krems, and K. W. Madison (to be published).
[25] J. Scherschligt, J. A. Fedchak, Z. Ahmed, D. S. Barker, K. Douglass, S. Eckel, E. Hanson, J. Hendricks, N. Klimov, T. Purdy, J. Ricker, R. Singh, and J. Stone, J. Vac. Sci. Technol. A **36**, 040801 (2018).
[26] V. B. Makhalov, K. A. Martiyanov, and A. V. Turlapov, Metrologia **53**, 1287 (2016).
[27] C. Makrides, D. S. Barker, J. A. Fedchak, J. Scherschligt, S. Eckel, and E. Tiesinga, Phys. Rev. A **99**, 042704 (2019).
[28] G. F. Gribakin and V. V. Flambaum, Phys. Rev. A **48**, 546 (1993).
[29] E. Bodo, F. A. Gianturco, N. Balakrishnan, and A. Dalgarno, J. Phys. B **37**, 3641 (2004).
[30] A. O. G. Wallis, E. J. J. Longdon, P. S. Ź uchowski, and J. M. Hutson, Eur. Phys. J. D **65**, 151 (2011).
[31] T. V. Tscherbul, in *Cold Chemistry: Molecular Scattering and Reactivity near Absolute Zero* (Royal Society of Chemistry, London, 2018), Chap. 6.
[32] I. Kozyryev, L. Baum, K. Matsuda, B. L. Augenbraun, L. Anderegg, A. P. Sedlack, and J. M. Doyle, Phys. Rev. Lett. **118**, 173201 (2017).

[33] S. Truppe, H. J. Williams, M. Hambach, L. Caldwell, N. J. Fitch, E. A. Hinds, B. E. Sauer, and M. R. Tarbutt, Nat. Phys. **13**, 1173 (2017).
[34] M. Mayle, B. P. Ruzic, and J. L. Bohn, Phys. Rev. A **85**, 062712 (2012).
[35] J. M. Hutson and P. Soldán, Int. Rev. Phys. Chem. **26**, 1 (2007).
[36] S. N. Vogels, T. Karman, J. Kłos, M. Besemer, J. Onvlee, A. van der Avoird, G. C. Groenenboom, and S. Y. T. van de Meerakker, Nat. Chem. **10**, 435 (2018).
[37] M. D. Frye, P. S. Julienne, and J. M. Hutson, New J. Phys. **17**, 045019 (2015).
[38] M. Lara, J. L. Bohn, D. Potter, P. Soldán, and J. M. Hutson, Phys. Rev. Lett. **97**, 183201 (2006).
[39] A. O. G. Wallis and J. M. Hutson, Phys. Rev. Lett. **103**, 183201 (2009).
[40] T. V. Tscherbul, J. Kłos, and A. A. Buchachenko, Phys. Rev. A **84**, 040701(R) (2011).
[41] P. S. Żuchowski and J. M. Hutson, Phys. Chem. Chem. Phys. **13**, 3669 (2011).
[42] J. Cui and R. V. Krems, Phys. Rev. A **88**, 042705 (2013).
[43] Y. V. Suleimanov and T. V. Tscherbul, J. Phys. B **49**, 204002 (2016).
[44] M. Morita, M. B. Kosicki, P. S. Żuchowski, and T. V. Tscherbul, Phys. Rev. A **98**, 042702 (2018).
[45] M. Morita, J. Kłos, A. A. Buchachenko, and T. V. Tscherbul, Phys. Rev. A **95**, 063421 (2017).
[46] See Supplemental Material at http://link.aps.org/supplemental/10.1103/PhysRevLett.123.013401, which includes Refs. [47–51], for details of numerical calculations and convergence tests.
[47] M. Tomza, C. P. Koch, and R. Moszynski, Phys. Rev. A **91**, 042706 (2015).
[48] M. D. McKay, R. J. Beckman, and W. J. Conover, Technometrics **21**, 239 (1979).
[49] M. Stein, Technometrics **29**, 143 (1987).
[50] L. M. C. Janssen, P. S. Żuchowski, A. van der Avoird, J. M. Hutson, and G. C. Groenenboom, J. Chem. Phys. **134**, 124309 (2011).
[51] L. M. C. Janssen, P. S. Żuchowski, A. van der Avoird, G. C. Groenenboom, and J. M. Hutson, Phys. Rev. A **83**, 022713 (2011).
[52] T. V. Tscherbul and A. Dalgarno, J. Chem. Phys. **133**, 184104 (2010).
[53] M. L. González-Martínez and J. M. Hutson, Phys. Rev. Lett. **111**, 203004 (2013).
[54] Y. Liu, M. Vashishta, P. Djuricanin, S. Zhou, W. Zhong, T. Mittertreiner, D. Carty, and T. Momose, Phys. Rev. Lett. **118**, 093201 (2017).
[55] W. H. Miller, J. Chem. Phys. **52**, 543 (1970).